INTERFACE SCIENCE 1, 31–47 (1993).

Interfacial Segregation in Ag-Au, Au-Pd, and Cu-Ni Alloys: II. [001] $\Sigma 5$ Twist Grain Boundaries

H.Y. WANG, R. NAJAFABADI, AND D.J. SROLOVITZ
Department of Materials Science and Engineering, University of Michigan, Ann Arbor, MI 48109

R. LESAR
Theoretical Division, Los Alamos National Laboratory, Los Alamos, NM 87545

Received August 9, 1992; Revised December 15, 1992.

Keywords: Grain boundaries, computer simulation, free energy, segregation.

Abstract. Atomistic simulations of segregation to [001] $\Sigma 5$ twist boundaries in Cu-Ni, Au-Pd, and Ag-Au alloy systems have been performed for a wide range of temperatures and compositions within the solid solution region of these alloy phase diagrams. In addition to the grain boundary segregation profiles, grain boundary free energies, enthalpies, and entropies were determined. These simulations were performed within the framework of the free energy simulation method, in which an approximate free energy functional is minimized with respect to atomic coordinates and atomic site occupation. For all alloy bulk compositions ($0.05 \leq C \leq 0.95$) and temperatures ($400 \leq T$ (K) $\leq 1{,}100$) examined, Cu and Au segregates to the boundary in the Cu-Ni and Au-Pd alloy systems, respectively; although in the Ag-Au alloys, the majority element segregates to the boundary. The width of the segregation profile is limited to approximately three to four (002) atomic planes. The classical theories for the segregation, and the effects of the relaxation with respect to either the atomic positions or the atomic concentrations, are discussed. The boundary thermodynamic properties depend sensitively on the magnitude of the boundary segregation, and some of them are shown to vary linearly with the magnitude of the grain boundary segregation.

1. Introduction

As a continuation of Part I, in this work, we apply the free energy simulation method to the calculation of the structure, composition, and thermodynamic properties of $\Sigma 5$ [001] twist boundaries in Ag-Au, Au-Pd, and Cu-Ni alloys. We find that many properties, such as the boundary free energies, the degree of segregation, the oscillatory behavior of composition profile, and even the segregant species, can be dramatically different from that of (100) free surfaces.

The segregation driving force is principally the same for all the types of defects, namely, the difference in the free energy of the system when a foreign atom is located at a defect and when the same atom is dissolved in bulk. Different defects have different structural properties, and therefore the driving forces and degree of segregation vary. Although grain boundaries and free surfaces have a great deal in common, as pointed out by Hondros and Seah [1], a high-angle boundary can be crudely described as mixture of free surface-like and bulk-like segments. Nonetheless, grain boundaries typically have much more complicated structures than either the bulk or surface and, therefore, it is more difficult to formulate meaningful segregation models. The classical segregation theories simply ignore the complexity of the boundary

structure, except in as much as it changes the heat of segregation.

Since McLean [2] estimates the heat of segregation ΔG from the complete release of the elastic strain energy of the solute when it segregates to the boundary, the resultant predictions are completely independent of the boundary structure. The strain energy E_{el} is calculated by equation (5) in Part I. Elastic strain energies estimated in this way are the same for both free surfaces and grain boundaries, and are generally correct to within a factor of two. To achieve higher accuracy, Seah and Hondros [1] employed the Brunauer, Emmett, and Teller (BET) gas adsorption theory [3] to write the solid-state analogue of the McLean adsorption isotherm as [4]

$$\frac{C_1}{1-C_1} = \frac{C_B}{C_B^0} \exp\left(-\frac{\Delta G'}{kT}\right) \tag{1}$$

where C_B^0 is the solute solubility, which can be taken from phase diagram of binary systems, and $\Delta G'$ is the free energy difference between the solute at the grain boundary and in equilibrium with a precipitate.

Both the McLean-Langmuir equation and the truncated BET theory are most appropriate for dilute interfacial and bulk concentrations. At higher segregation levels, however, interaction of segregating atoms can be very significant and, in many cases, is the major cause of marked deviations from ideal Langmuir-McLean behavior. These deviations can be described by the Fowler-adsorption equation [5], which introduces an interaction term ε between two neighboring solute atoms. If Z_1 is the local coordination number, then the Fowler heat of segregation is given as

$$\Delta G = \Delta G_0 + 2Z_1\varepsilon C_1 \tag{2}$$

where ΔG_0 is a constant and is independent of the segregation level. When the solute concentration is locally very small, the second term in equation (2) can be ignored, and the Fowler-adsorption reduces to the McLean model.

Although the Fowler-adsorption model accounts for solute interaction in a simple way, another major source of error in the classical McLean segregation analysis is left uncorrected: i.e., the assumption that all boundary sites are equivalent. Vitek and Wang [6] pointed out that the grain boundary segregation is very anisotropic, and the heat of segregation can be substantially different from one atomic site to another. Therefore, the average heat of segregation determined from equation (2) can not provide an accurate estimate of segregation behavior in any but the simplest cases.

To obtain the structure of a grain boundary, the effects of boundary structure on segregation, and the microscopic distribution of solute at the boundary, it is necessary to perform atomistic simulations. Early atomistic simulations of segregation were based upon static relaxation methods in systems with single solute atoms at zero temperature [6]. Many aspects of the relationship between the structure and segregation were revealed by this method. However, the magnitude of the segregation can not be determined by such a static simulation method. Monte Carlo simulation methods (discussed in Part I), on the other hand, have allowed atomistic simulations to be extended to alloys systems where the local composition can change during the course of the simulation. Unfortunately, such methods requires substantial computational resources, and do not provide such basic segregation thermodynamic properties as the free energy of segregation. The recently introduced free energy minimization method [7–10 in part I], on the other hand, is computationally efficient, provides thermodynamic data, and yields segregation results that are in excellent agreement with Monte Carlo data [8, 8(*a*), 9]. Although this approach is inherently less accurate than the Monte Carlo method, its efficiency allows systematic evaluations of trends in interfacial and segregation thermodynamics as a function of the pertinent experimental parameters such as temperature and bulk composition. The most important feature of this method is that it yields a simple expression for the finite-temperature free energy of the system. Minimizing the free energy with respect to the positions and concentrations of the atomic sites produces the equilibrium atomic structures and free energies, from which all other thermodynamic quantities may be derived.

The present paper focuses on grain boundary segregation in the same three alloy systems (Ag-

Au, Au-Pd, and Cu-Ni) examined in a previous study of surface segregation (Part I). We chose to consider the [001] Σ5 twist boundary in this study, since it (1) is a high angle boundary; (2) has the same interface plane as in the surface study; and (3) has a short period, which is important to limit the computational burden. We examine the [001] Σ5 twist boundary in the Ag-Au, Au-Pd, and Cu-Ni systems as a function of temperature and bulk composition. The segregation profiles and segregation thermodynamics are determined self-consistently with the atomic structure of the boundary. The relationships between segregation behavior of these three different alloy systems and the relationship between the [001] Σ5 twist boundary and the (001) free surface are considered in some detail.

Since the basic simulation procedure was outlined in Part I (previous paper) of this study, the details are not repeated here. The geometry of the simulation block used in the grain-boundary simulations is the same as that employed in our earlier studies of grain boundaries [7–9]. The Σ5 grain boundary was created by cutting a single crystal along an (001) plane and rotating about a common [100] axis by 36.9°. The simulations were performed using 2×2 arrays of the basic Σ5 period or unit cell with a total of 20 atoms per (002) plane. To make the calculation more efficient, the simulation started with only four (002) planes (two planes on each side of the grain boundary), and the number of atomic planes was varied such that increasing the number of atomic planes did not change the grain boundary free energy to within the convergence criterion. This typically required ~12 atomic planes on each side of the boundary.

2. Results

Simulations based upon the free energy simulation method were performed on [001] Σ5 twist boundaries in Cu-Ni, Au-Pd, and Ag-Au alloys for temperatures between 400 and 1,100 K. At each temperature, between 13 and 19 different bulk compositions were examined. The temperatures and compositions examined in this study are all within the continuous solid solution region of the phase diagrams of the three alloys, as determined from perfect crystal free energy simulation results using the same EAM potentials [11].

The thermodynamic properties of the defects are distinguished from the bulk properties by the subscripts B or gb, where B represents bulk (solid solution) crystal properties, and gb refers to grain boundary properties. The grain boundary properties are defined as the difference between the property of the bicrystal and that of a random solid solution with the same number of atoms at the same chemical potential difference and temperature: $X_{gb} = [X(\text{bicrystal}) - X_B]/A$, where X is the thermodynamic property of interest (e.g. free energy, enthalpy, etc.), and the grain boundary properties have been normalized by the grain boundary area A. The grain boundary properties may be calculated in two limits. The first is the unsegregated limit, as may be found by quenching the sample from very high temperature (where segregation is negligible) to the temperature of interest, and its properties are denoted by $X_{gb,u}$. The second limit corresponds to equilibrium segregation at the temperature of interest, and is denoted by $X_{gb,s}$. The change in the thermodynamic properties that may be associated with the segregation is given by the difference between these two values, i.e., $\Delta X_{gb} = X_{gb,s} - X_{gb,u}$.

Following segregation, the concentration profile in the bicrystal is not uniform, and the mean (dimensionless) concentration on the (002) planes parallel to the boundary are given by C_n, where the subscript n denotes the plane number [e.g., C_3 is the mean concentration in the third (002) plane from the boundary]. We adopt the notation C_B as the dimensionless bulk concentration far from the grain-boundary plane. Throughout this paper, all concentrations $0 \leq C \leq 1$ will refer to the Cu concentration for Cu-Ni alloys, Au for Au-Pd, and Ag for Ag-Au alloys; the concentrations for the other components of these binary alloys are given simply by 1-C. The degree of segregation, or *excess* concentration, is given by the difference between the concentration on the plane and the bulk concentration, and is denoted $C_{n,xs}$. The net or *total excess* segregation is the sum of $C_{n,xs}$ over all (002) planes, and is referred to as $C_{T,xs} = \sum_{n=1}^{\infty} C_{n,xs}$. The expression $C_{T,xs}$ is nonzero here, since the present simulations were performed in the grand

canonical ensemble, while in either the canonical or microcanonical ensemble $C_{T,xs} = 0$. It is useful to note that the concentration $C_{T,xs}$, as defined above, only accounts for one side of the boundary. Since the boundary has two sides, the *physical* total excess concentration is twice as large as the reported $C_{T,xs}$.

2.1. Segregation Profiles

The concentration profiles in the vicinity of the [001] $\Sigma 5$ twist boundary for Cu-Ni, Au-Pd, and Ag-Au alloys are shown in figure 1 at $T = 600$ K and different bulk concentrations C_B. When the bulk concentration C_B is varied from 20% to 80% Cu in the Cu-Ni system, the Cu concentration at the (002) plane closest to the boundary ($n = 1$) varies from 64% to 95%. The second (002) plane from the boundary ($n = 2$) also exhibits Cu segregation, although to a much smaller degree than the first (002) plane, which is different from the surface where Ni segregates to the second layer (Part I). By the third (002) plane from the boundary ($n = 3$), the Cu concentration is nearly equal to the bulk concentration. These segregation profiles indicate that in the Cu-Ni system, the effective width of the grain boundary segregation profile is approximately four (002) planes (i.e., two on either side of this boundary).

In the Au-Pd alloys (Fig. 1(*b*)), the concentration profile exhibits a similar form as that seen in the Cu-Ni alloys, only the degree of segregation is smaller. When the bulk concentration of Au increases from 20% to 80%, the first two (002) planes are enriched in Au, although the second plane shows a much smaller degree of Au segregation. On the third plane, however, there is a very small Pd enrichment. The effective width of the grain boundary segregation profile is also approximately four (002) planes (two on either side of this boundary). The main difference between the shape of the concentration profiles in Cu-Ni and Au-Pd alloys is that the first layer Cu segregation in Cu-Ni alloys is much stronger than that of Au in Au-Pd alloys.

In the Ag-Au system (Fig. 1(*c*)), the magnitude of the segregation is very small, and the segregation pattern is quite different from that of the Cu-Ni and Au-Pd alloys. For bulk concentrations of 20% and 40% Ag, the first (002) plane is enriched in Au, while for bulk Ag concentrations of 60% and 80%, the first plane is enriched in Ag. The second (002) plane is enriched in Ag over the whole concentration range. Again, by the third plane, the concentration is almost equal to that of the bulk concentration, and the effective width of the grain boundary segregation profile is also four (002) planes.

The effects of temperature and bulk concentration on the first-layer segregation may be seen more clearly in Fig. 2, where we plot C_1 as a function of the bulk concentration for different temperatures. In this type of plot, the straight line $C_1 = C_B$ corresponds to zero segregation. Clearly, $C_1 = 0$ in the limit that C_B goes to zero and C_1 must go to unity as C_B approaches one, since in these limits no solute is present. For the Cu-Ni and Au-Pd alloys, the same element segregates for all T and C_B examined (Cu in Cu-Ni and Au in Au-Pd). The Cu-Ni alloy exhibits stronger segregation than Au-Pd. The main effect of temperature is simply to reduce the magnitude of the segregation. In the Ag-Au alloys, however, the magnitude of segregation is very small. The C_1 curves do not show much deviation from $C_1 = C_B$ line, however, careful examination shows that when the bulk concentration is Au-rich, the Au concentration at the boundary is enhanced above the bulk value, although when C_B corresponds to a Ag-rich alloy, Ag segregates to the boundary plane. The effect of the temperature is small, and increases the boundary Ag concentration over the whole bulk concentration region.

The magnitude of the segregation in the three alloy systems may be seen more clearly in figure 3, where we plot the excess concentration of the first (002) plane as a function of the bulk concentration at $T = 600$ K. In this type of plot, $C_{1,xs}$ must go to zero as the bulk concentration goes to zero or one. In the Ag-Au alloys, it is now clear that at Au-rich side $C_{1,xs}$ is negative and at Ag-rich side $C_{1,xs}$ is positive, implying that it is enriched in Au at Au-rich side and enriched in Ag at Ag-rich side. The maximum segregation in the Cu-Ni, Au-Pd, and Ag-Au alloys occurs at approximately 0.45, 0.1, and 0.01 at 600K, respectively. Based upon this observation, we conclude that segregation is more ideal

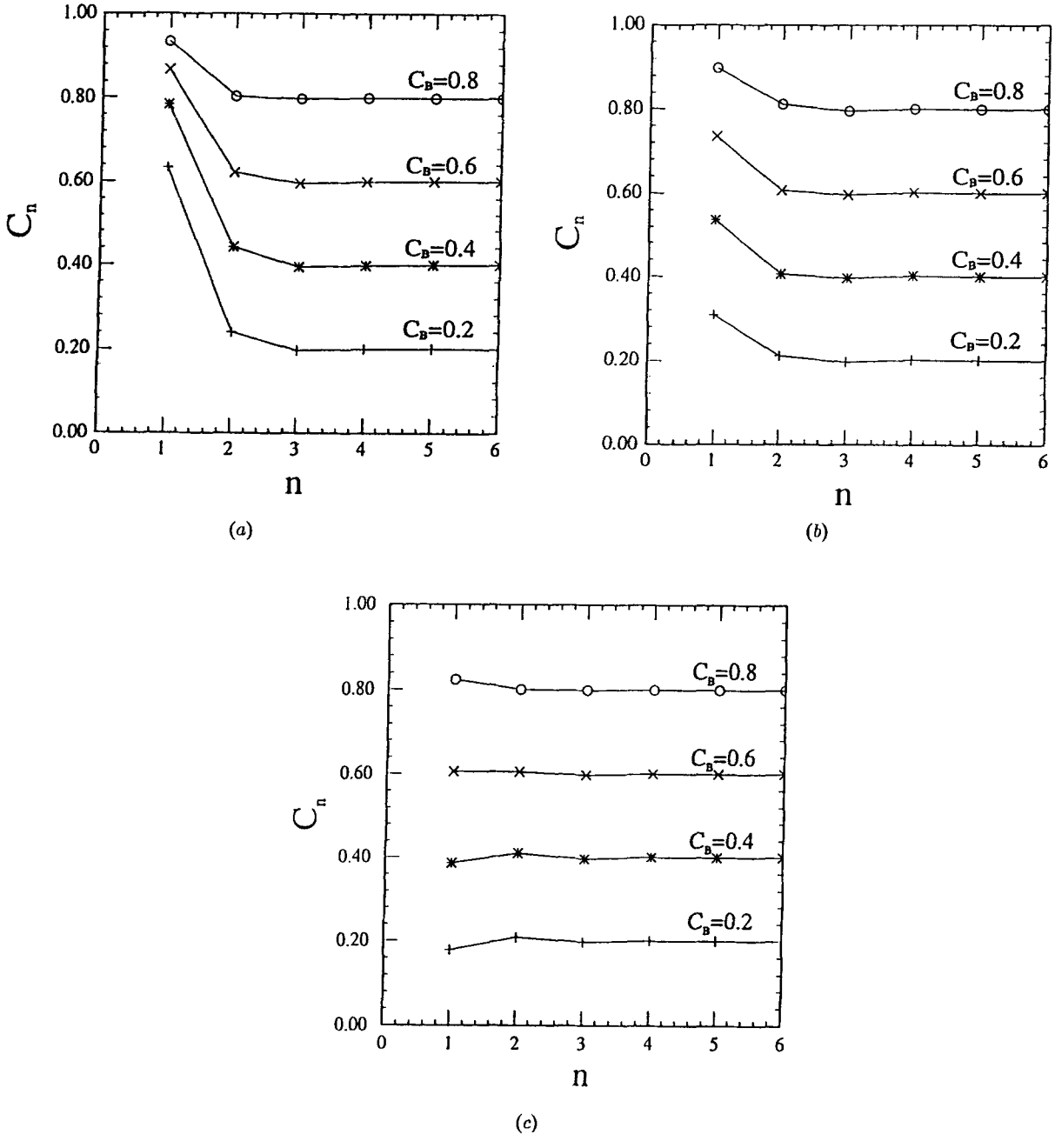

Fig. 1. Concentration C_n averaged over atomic planes parallel to the grain boundary versus layer number, n, where $n = 1$ corresponds to the (002) plane adjacent to the boundary with (*a*) for the Cu-Ni; (*b*) for Au-Pd; and (*c*) for Ag-Au alloys. The temperature is 600 K.

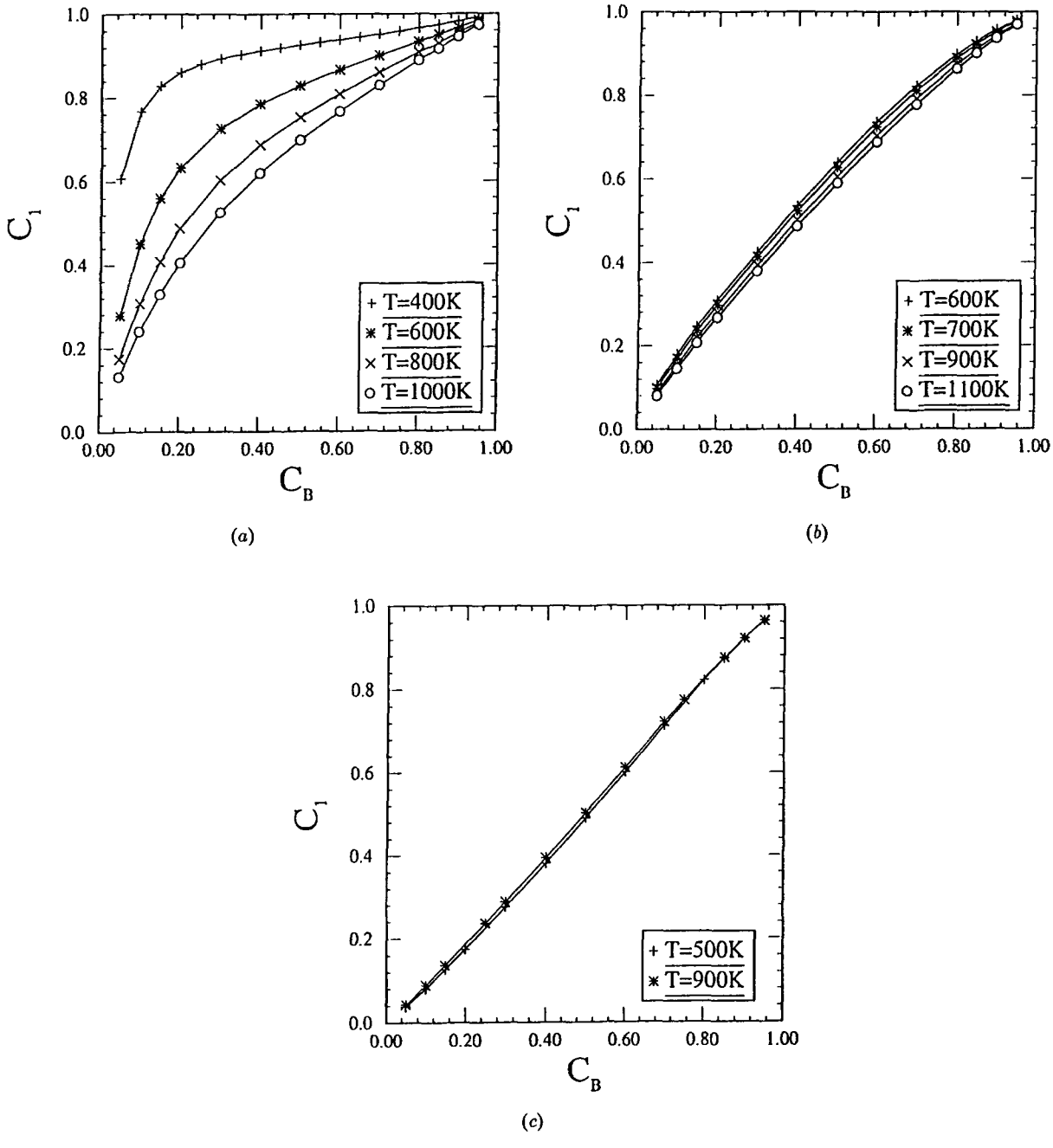

Fig. 2. The concentrations at the first layer C_1 plotted as a function of the bulk concentration C_B. (*a*) is for Cu-Ni; (*b*) is for Au-Pd; and (*c*) is for Ag-Au alloys.

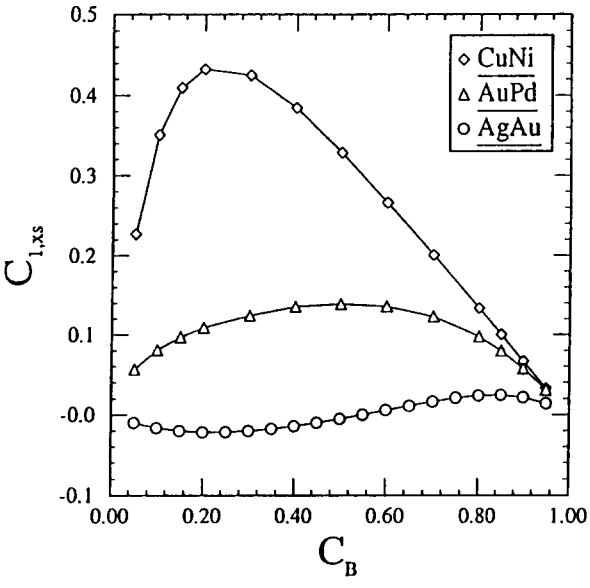

Fig. 3. The excess concentration at the first (002) plane versus the bulk concentration C_B at 600 K. The diamond, triangle, and circle are for Cu-Ni, Au-Pd, and Ag-Au alloys, respectively.

in Cu-Ni than in either of the other two alloy systems.

2.2. Boundary Free Energy

The grain boundary free energy in the grand canonical ensemble is denoted as $\Gamma_{gb} = (\Omega_{gb} - \Omega_B)/A$, where Ω_{gb} is the grand potential of the system with the grain boundary, Ω_B is the grand potential for the perfect crystal, and A is the area of the grain boundary. Γ_{gb} is plotted as a function of bulk concentration C_B in figure 4. The Γ_{gb} curves are usually quite complicated. The complexity is introduced by the competition between the various terms that make up the free energy: enthalpy, entropy and chemical potentials. The lower the temperature, the smaller the contribution to the free energy from the entropy, such that Γ_{gb} is larger. However, the lower the temperature, the more negative the contribution from the energy that drives segregation and, hence, the smaller the magnitude of Γ_{gb}.

For bulk Cu concentrations less than approximately 0.5 in the Cu-Ni alloys (Fig. 4(*a*)), Γ_{gb} is smallest at the lowest temperature studied (T = 400 K). For $C_B > 0.5$, the smallest grain boundary free energy is found at the highest temperature studied (T = 1,000 K). These results, similar to the surface segregation in Cu-Ni, may be understood by considering the effects of bulk concentration and temperature on the segregation behavior (see figure 2(*a*). The degree of Cu segregation is greatest at low temperatures and for bulk concentrations on the Ni-rich side of the phase diagram. In this regime (low T, small C_B), where the degree of segregation is a maximum, Γ_{gb} is a minimum. On the other hand, at high T and large C_B, the degree of segregation is small. In this regime, the ordering of the different temperature curves in the Γ_{gb} versus C_B plot are as they are in the absence of segregation.

In the Au-Pd and Ag-Au alloys (Fig. 5(*b*) and (*c*)), since the segregation is not as strong as that in Cu-Ni alloys, the grain boundary free energy curves are relatively simple and similar to that in the unsegregated case. The contribution to the free energy from the entropy term dominates the contribution from the other terms, such that the effect of increasing the temperature on the boundary free energy curves is simply to shift these curves to lower values of Γ_{gb}. The boundary free energy of both the Cu-Ni and the Au-Pd alloys decreases monotonically as C_B increased. While in the Ag-Au alloys, there is a maximum value in the boundary free energy curve, and it is this maximum in the boundary free energy curve where the segregation reverses its direction as the bulk concentration varies from zero to one, as discussed below.

The effect of segregation on the boundary free energy Γ_{gb} may be seen more clearly in figure 5, where Γ_{gb} is plotted as a function of bulk concentration C_B for the boundaries with (solid curves) and without (dotted curves) the segregation for the three alloy systems at T = 600 K. When segregation is allowed to occur, the grand potential is minimized with respect to the position and the concentration of each site, while for the unsegregated grain boundary, the compositions of each site are fixed at C_B, and the grand potential is minimized only with respect to the atomic coordinates. In the Cu-Ni and Au-Pd alloys, the unsegregated boundary free energy $\Gamma_{gb,u}$ varies

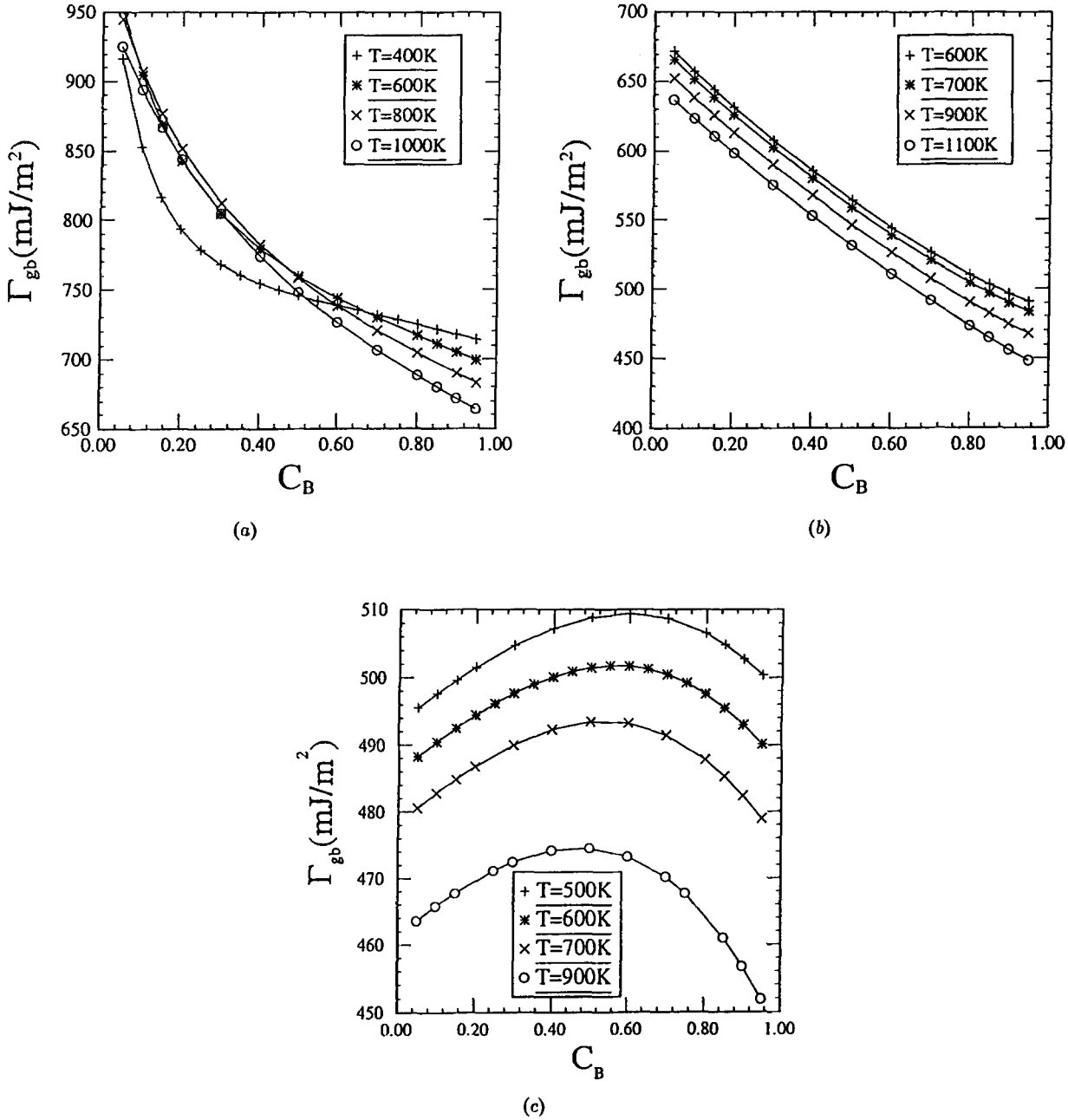

Fig. 4. The grain boundary free energy versus bulk concentration C_B at four different temperatures. (*a*) Cu-Ni alloys; (*b*) Au-Pd alloys; and (*c*) Ag-Au alloys.

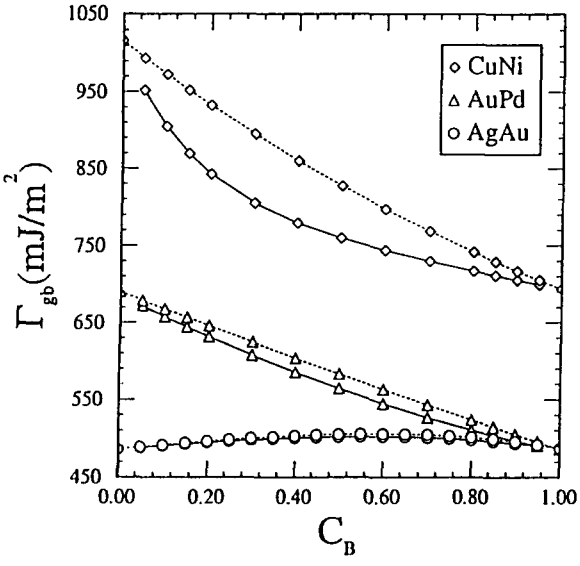

Fig. 5. The boundary free energy is plotted as a function of the bulk concentration at 600 K. The solid lines are for the segregated boundary, and the dashed lines are for the unsegregated boundary. The diamonds, triangles, and circles correspond to Cu-Ni, Au-Pd, and Ag-Au alloys, respectively.

in a nearly linear manner with the bulk concentration C_B, and the $\Gamma_{gb,u}$ versus C_B curves are approximately linear interpolations between the Γ_{gb} values of the two pure elements in the alloys. In the Ag-Au alloys, however, $\Gamma_{gb,u}$ has a maximum around the 50% bulk concentration. The difference between the solid and the dotted lines, or the effect of the segregation on the boundary free energy, is the largest in the Cu-Ni alloys and is the smallest in the Ag-Au alloys, which is consistent with the degree of the segregation in these three alloys (see figure 3).

3. Discussion

In the previous section, we reported several effects of segregation to the [001] Σ5 twist boundary in Cu-Ni, Au-Pd, and Ag-Au alloys as a function of both temperature and composition. We noted that, as in the free surfaces (Part I), there is a correlation between the excess concentration and the change of the boundary free energy from segregated boundaries to unsegregated boundaries. To investigate the nature of the correlations between segregation and boundary properties, we focus on that part of the thermodynamic properties that depends on the segregation per se; that is, the difference between the thermodynamic properties with and without segregation. It is important to look at this difference so as not to bias the results with intrinsic properties of the boundary (e.g., there is a grain boundary vibrational entropy even in pure materials).

For Cu-Ni alloys, figure 6(*a*) shows the excess grand potential $\Delta\Gamma_{gb}$ plotted against the total excess concentration $C_{T,xs}$. Similarly, Figs. 6(*b*)–(*d*) show the excess vibrational entropy $\Delta S_{gb,v}$, the excess enthalpy ΔH_{gb}, and the excess boundary expansion ΔD_{gb} (i.e., the excess grain boundary volume per unit area) as functions of the total excess concentration $C_{T,xs}$. These plots contain data taken over the entire ranges of temperature and concentration reported in the previous section. In all four cases, we find that there is a very good linear proportionality between these grain boundary thermodynamic properties and the total excess concentration. Linear numerical fits to this data show that $\Delta X_{gb} = mC_{T,xs}$, with the proportionality constant $m = -200.25 \pm 1.76\, mJ/m^2$ for $\Delta\Gamma_{gb}$, $0.451 \pm 0.001\, mJ/m^2K$ for $\Delta S_{gb,v}$, $4,271.2 \pm 12.2\, mJ/m^2$ for ΔH_{gb}, 0.1752 ± 0.0004 Å for ΔD_{gb}. The linear dependence of these four thermodynamic quantities on the total excess concentration implies that the effects of segregation on the thermodynamic properties is simply proportional to the degree of segregation.

For Au-Pd alloys, the excess grand potential $\Delta\Gamma_{gb}$, the excess vibrational entropy $\Delta S_{gb,v}$, and the excess boundary expansion ΔD_{gb} are plotted as functions of the total excess concentration $C_{T,xs}$, in figure 7. As in the surface of the Au-Pd alloys (Part I), the excess grand potential, the excess vibrational entropy, and the excess boundary expansion are linear functions of the total excess concentration for all C_B and T. If we fit these data to a linear equation $\Delta X_{gb} = mC_{T,xs}$, we find $m = -127.1 \pm 2\, mJ/m^2$, $0.448 \pm 0.005\, mJ/m^2K$, and 0.492 ± 0.004 Å for $\Delta\Gamma_{gb}$, $\Delta S_{gb,v}$, and ΔD_{gb}, respectively. There is much more scatter of the data in the Au-Pd case than in the Cu-Ni alloy system. This is presumably due to the influence of the configurational entropy (symmetric around a concentration of 50% in the approxi-

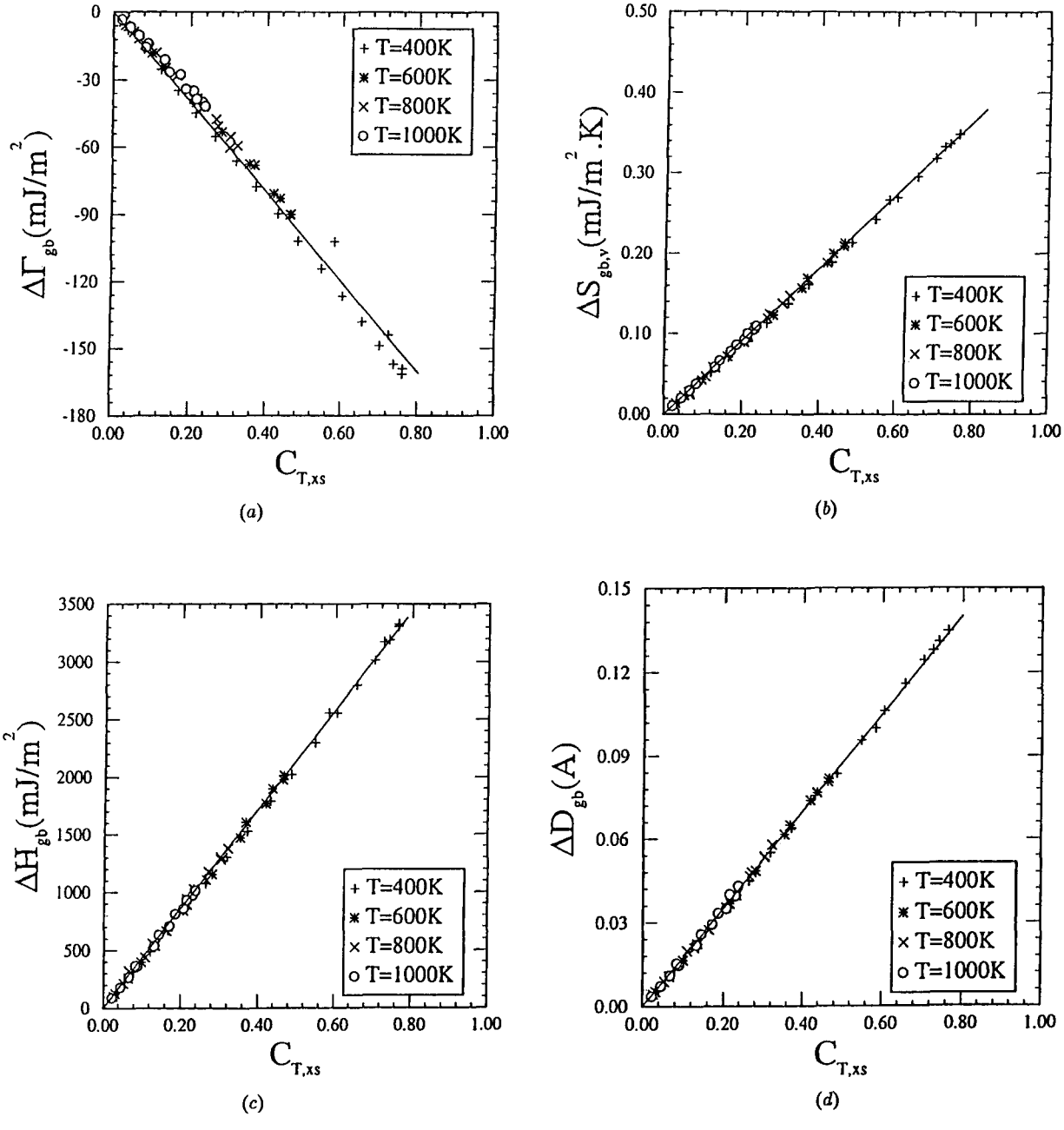

Fig. 6. The excess boundary free energy (*a*), excess boundary vibrational entropy (*b*), excess boundary enthalpy (*c*), and excess boundary thermal expansion (*d*) in Cu-Ni alloys versus the total excess concentration. The plus, asterisk, cross, and circle are for 400, 600, 800, and 1,000 K, respectively. The straight lines are fit to all of the data.

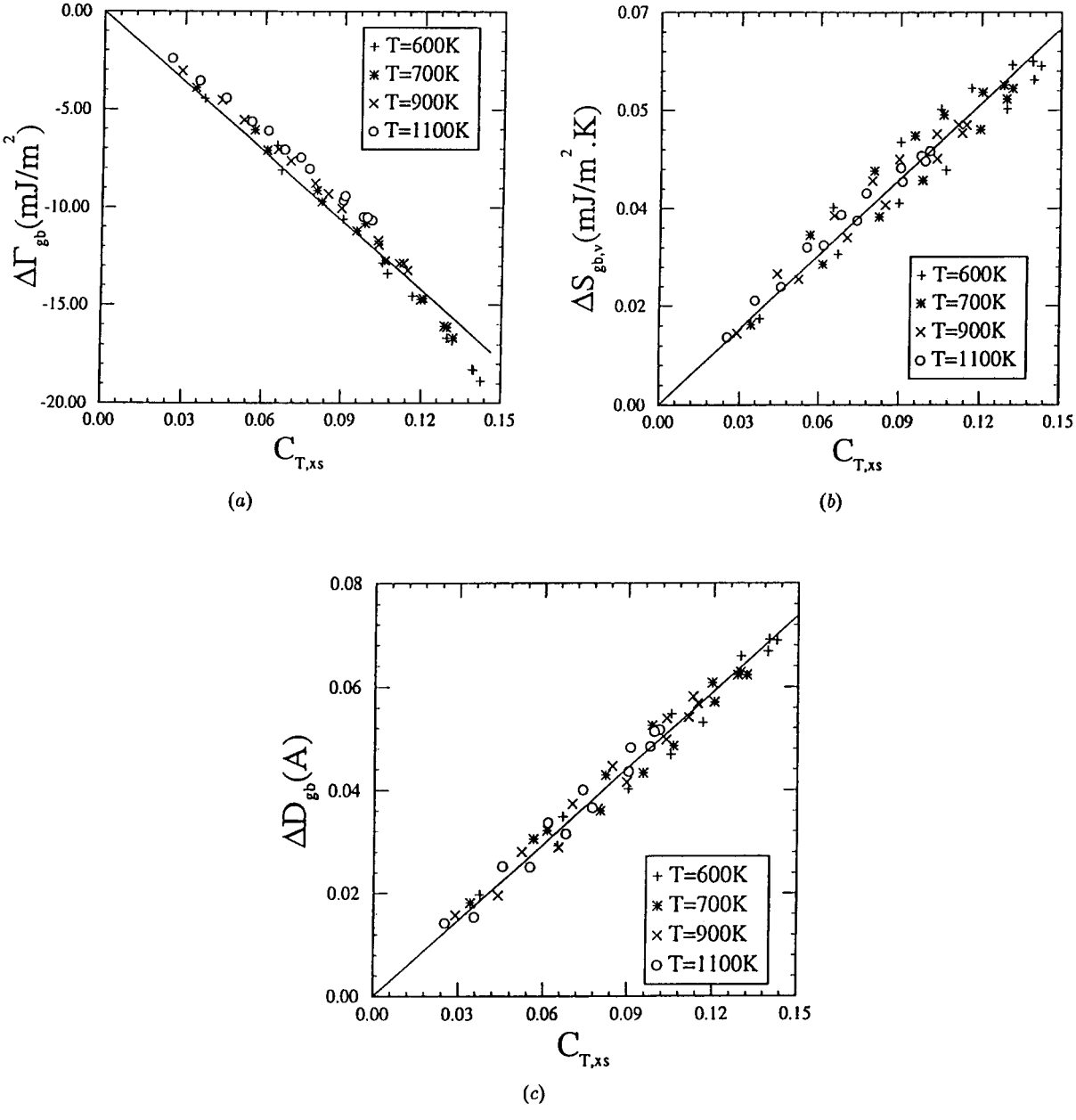

Fig. 7. The excess boundary free energy (*a*), excess boundary vibrational entropy (*b*), and excess boundary thermal expansion (*c*) in Au-Pd alloys versus the total excess concentration. The plus, asterisk, cross, and circle are for 600, 700, 900, and 1,100 K, respectively. The straight lines are fit to all of the data.

mation we employ), which does not scale linearly with excess concentration. The configurational entropy has a larger effect on the total free energy when the degree of segregation is weaker due to the decreased enthalpic contributions.

For Ag-Au alloys, the excess vibrational entropy $\Delta S_{gb,v}$, the excess enthalpy ΔH_{gb}, and the excess boundary expansion ΔD_{gb} are plotted as functions of the total excess concentration in figure 8. The excess concentration $C_{T,xs}$ is varied from about -0.02 to 0.03, and the order of the magnitude of $\Delta S_{gb,v}$ and ΔD_{gb} is only about 0.001. In these three plots, only the excess enthalpy ΔH_{gb} [Fig. 8(*b*)], shows a good linear behavior in terms of the total excess concentration. The other two excess quantities are quite scattered, particularly the excess entropy plot Fig. 8(*a*) with $C_{T,xs} > 0$. If we still fit these data to a linear equation $\Delta X_{gb} = mC_{T,xs}$, despite the scattering in the $\Delta S_{gb,v}$ and ΔD_{gb} data, we find $m = -0.211 \pm 0.006\, mJ/m^2K$ for $\Delta S_{gb,v}$, $4,238 \pm 35\, mJ/m^2$ for ΔH_{gb}, and 0.28 ± 0.01 Å for ΔD_{gb}. The same comments regarding the source of this scatter made with respect to the Cu-Ni versus the Au-Pd results apply even more so here.

Of all the (100) free surfaces (Part I) and the [001] twist boundaries of the three alloys, only in the Ag-Au alloy grain boundaries does the sign of the segregation reverse itself as the bulk concentration varies from zero to one. This may be understood by considering certain features of the boundary free energy versus bulk concentration C_B. According to the Gibbs [12] adsorption isotherm for binary alloys with very dilute impurity concentration

$$C_{1,xs} = -\frac{C_B}{KT}\frac{\partial \Gamma_{gb}}{\partial C_B} \tag{3}$$

The sign of the segregation depends upon the sign of the slope of the free energy versus bulk concentration curve. In the Ag-Au alloy systems (Fig. 4(*c*)), the free energy versus bulk concentration curve shows a maximum at approximately 0.5; hence, the slope of the curve changes its signs as C_B is varied. Therefore, the segregation changes sign as C_B goes from zero to one.

In the $\Sigma 5$ [001] twist boundaries, there are two independent sites on each (002) plane: coincidence lattice site (CS) and noncoincidence lattice site (NCS). These two sites have different atomic environment; therefore, they have different values of the heat of segregation and different degree of segregations. We plot the excess concentration of CS and NCS sites on the first (002) plane of the boundary at $T = 600$ K in Fig. 9. For Cu-Ni alloys (Fig. 9(*a*)), Cu segregates to both the CS and NCS sites, and the maximum excess concentration at the CS and NCS is about 0.54 and 0.4, respectively. For Au-Pd alloys (Fig. 9(*b*)), however, the excess concentration of Au is about 0.26 at the CS sites and 0.1 at the NCS sites. In the Ag-Au alloys (Fig. 9(*c*)), the segregating element at the CS and NCS sites can be different. The CS sites are always enriched in Ag, while the NCS sites are enriched in Ag for $C_B > \sim 0.8$ and enriched in Au for $C_B < \sim 0.8$.

In addition to the configurational entropy as a source of scatter in the excess thermodynamic properties versus bulk concentration plots, some of the scatter may be attributable to the difference between the segregation to the CS and the NCS sites. Because the segregation dependence of the thermodynamic properties are different for these two different atomic sites, and the magnitude of the relative excess concentration difference in Ag-Au alloys is the largest and in Cu-Ni alloys is the smallest, it is not surprising that the Ag-Au alloys show more scatter in the excess thermodynamic properties versus bulk concentration plots than do the other alloy systems.

As we have discussed in Part I, the exact expression for the magnitude of the segregation can be written as

$$\frac{C_i}{1-C_i} = \frac{C_B}{1-C_B}\exp\left[-\beta\left(\frac{\partial F}{\partial C_i} - \frac{\partial F}{\partial C_B}\right)\right] \tag{4}$$

where $\beta = 1/k_BT$; C_i is the concentration of site i; and F is the free energy of the system excluding the configurational entropy

$$F = E + A_v \tag{5}$$

For each plane, we have two different values of the heat of segregation: Q_C (evaluated as $\partial F/\partial C_C - \partial F/\partial C_B$) and Q_N (evaluated as $\partial F/\partial C_N - \partial F/\partial C_B$), where the subscripts C and N denote coincident CS and noncoincident NCS sites, respectively. The heats of segregation are

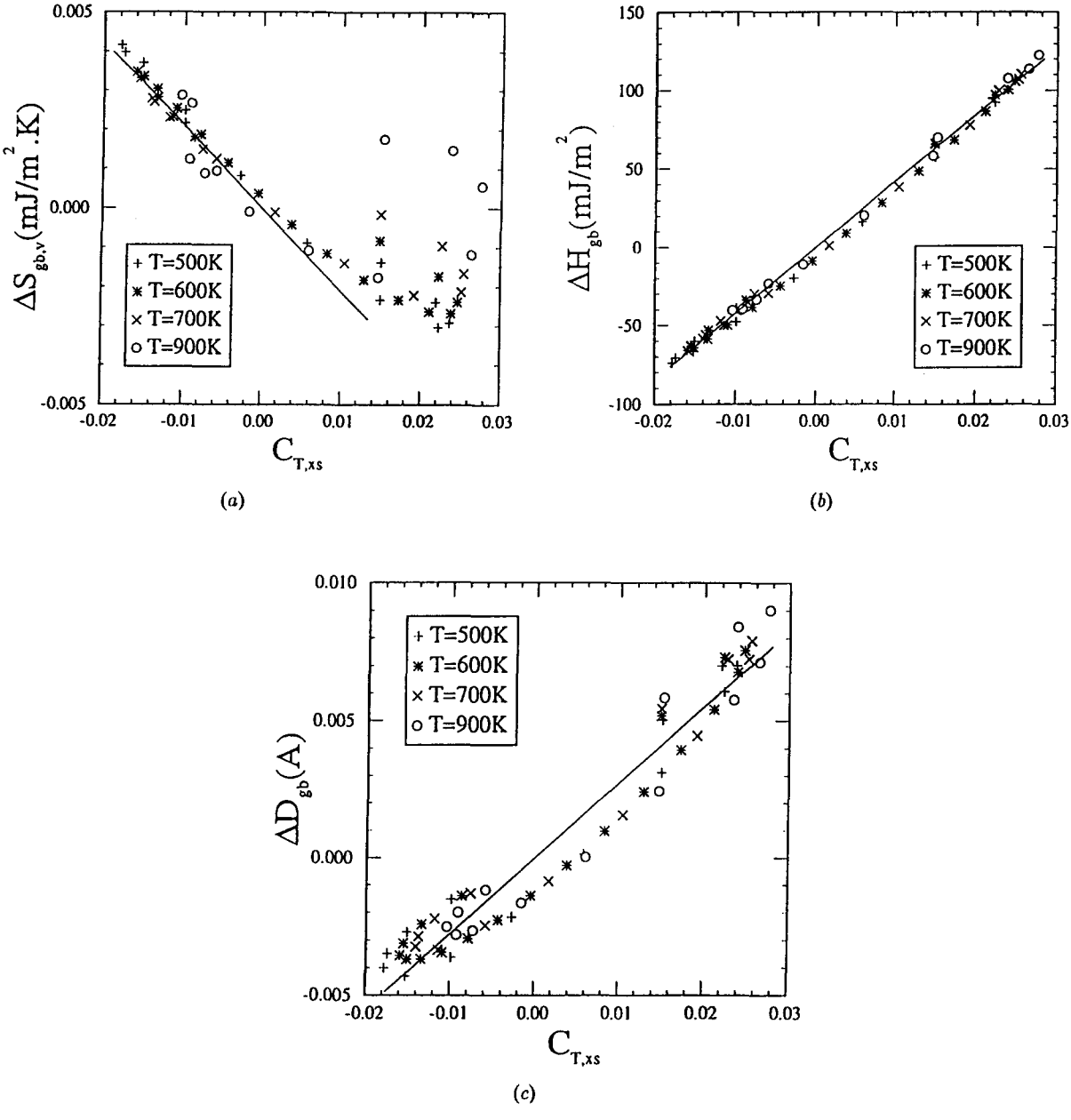

Fig. 8. The excess boundary vibrational entropy (*a*), excess boundary enthalpy (*b*), and excess boundary thermal expansion (*c*) in Ag-Au alloys versus the total excess concentration. The plus, asterisk, cross, and circle are for 500, 600, 700, and 900 K, respectively. The straight lines are fit to all of the data.

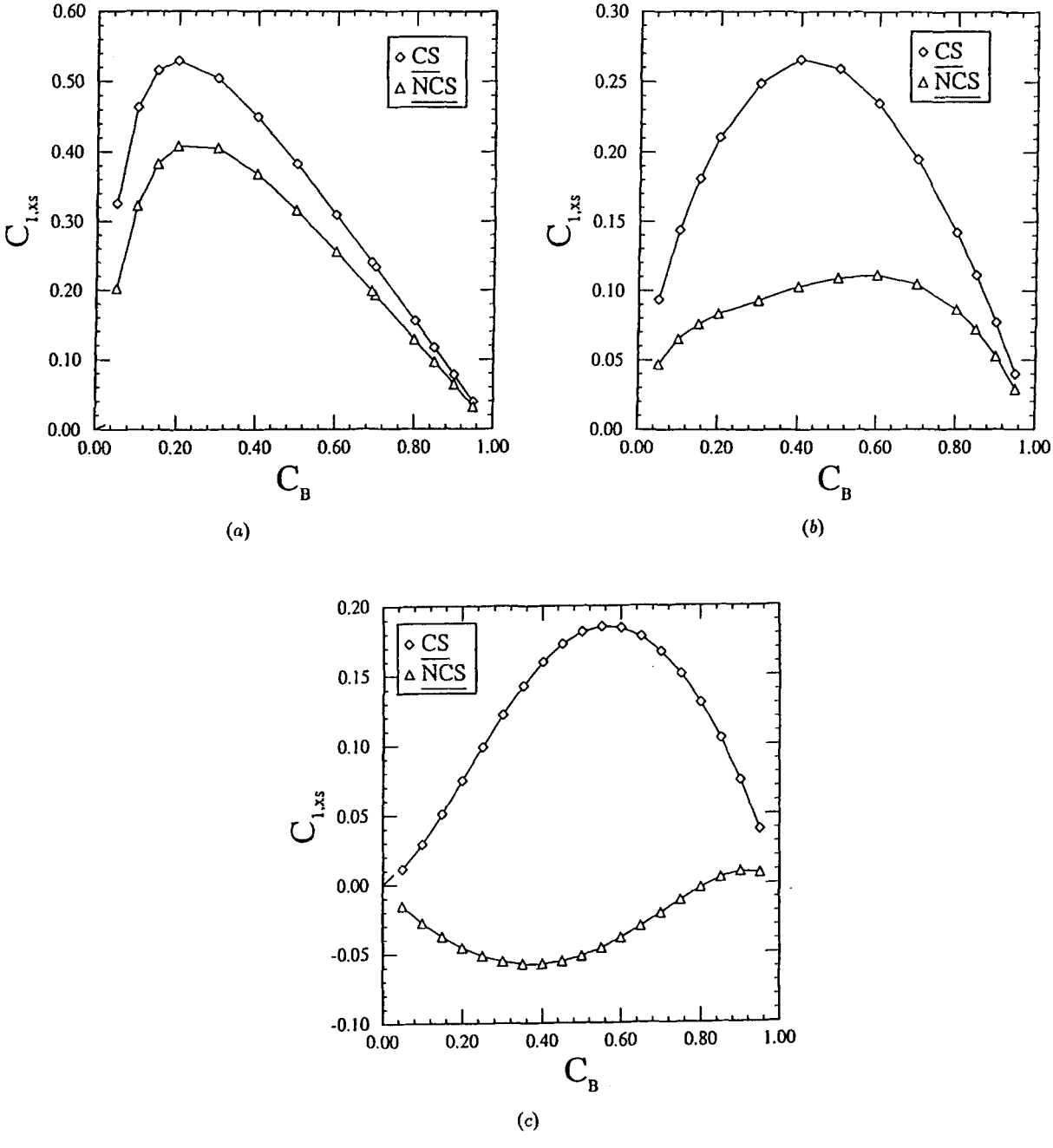

Fig. 9. The excess first layer concentration is plotted as a function of the bulk concentration. The diamonds are for the coincidence lattice sites, and the triangles are for the noncoincidence lattice sites. Figs. (*a*) Cu-Ni alloys; (*b*) Au-Pd alloys; and (*c*) Ag-Au alloys.

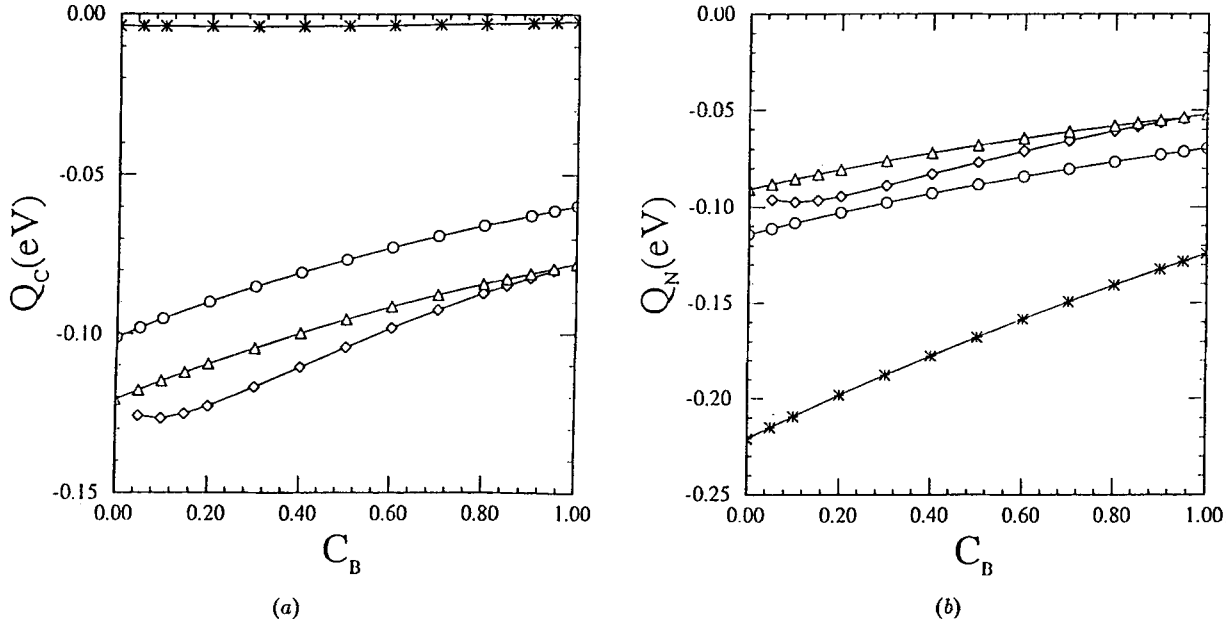

Fig. 10. The heat of segregation in Cu-Ni alloys for (*a*) the coincidence site $Q_C(= \partial F/\partial C_C - \partial F/\partial C_B)$ and for (*b*) the noncoincidence site $Q_N(= \partial F/\partial C_N - \partial F/\partial C_B)$ versus the bulk concentration C_B at $T = 600$ K. The diamonds correspond to the fully relaxed boundary, the triangles to the unsegregated boundary, the circles to the unrelaxed boundary with the same boundary expansion as the unsegregated one, and the asterisks to the totally unrelaxed boundary.

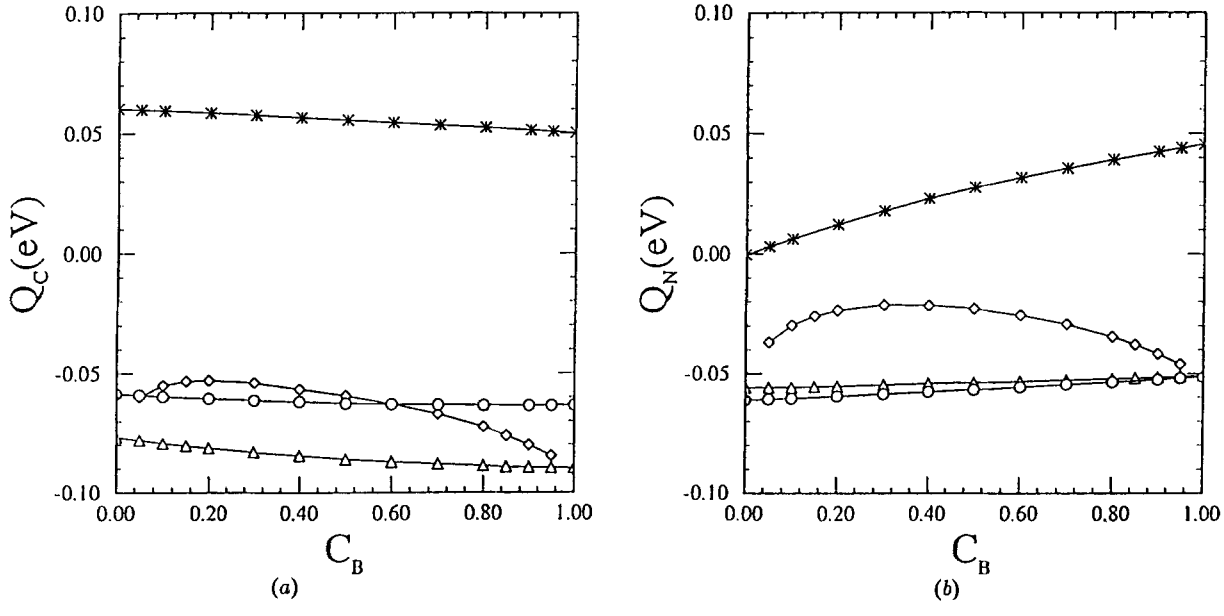

Fig. 11. The heat of segregation of Au-Pd alloys for (*a*) the coincidence site $Q_C(= \partial F/\partial C_C - \partial F/\partial C_B)$ and for (*b*) the noncoincidence site $Q_N(= \partial F/\partial C_N - \partial F/\partial C_B)$ versus the bulk concentration C_B at $T = 600$ K. The diamonds correspond to the fully relaxed boundary, the triangles to the unsegregated boundary, the circles to the unrelaxed boundary with the same boundary expansion as the unsegregated one, and the asterisks to the totally unrelaxed boundary.

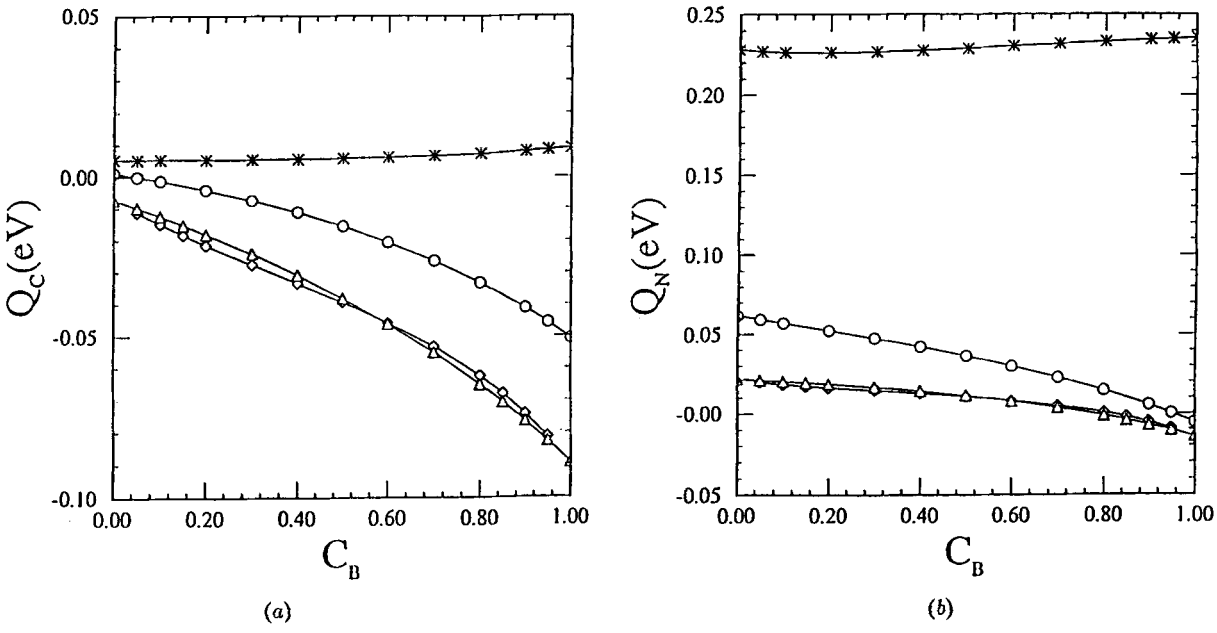

Fig. 12. The heat of segregation of Ag-Au alloys for (*a*) the coincidence site $Q_C(= \partial F/\partial C_C - \partial F/\partial C_B)$ and for (*b*) the noncoincidence site $Q_N(= \partial F/\partial C_N - \partial F/\partial C_B)$ versus the bulk concentration C_B at T = 600 K. The diamonds correspond to the fully relaxed boundary, the triangles to the unsegregated boundary, the circles to the unrelaxed boundary with the same boundary expansion as the unsegregated one, and the asterisks to the totally unrelaxed boundary.

plotted as functions of the bulk concentration C_B in figures 10–12 for Cu-Ni, Au-Pd, and Ag-Au alloys, respectively, for CS and for NCS. To evaluate the degree to which relaxation with respect to atomic position and concentration affect the heat of segregation, we have calculated the heat of segregation in four different limits: both atomic concentrations and positions relaxed (segregated boundary), only atomic positions relaxed (unsegregated boundary), unrelaxed but with the same volume expansion as the unsegregated boundary, and the totally unrelaxed boundary. In the present study, the totally unrelaxed boundary was created by cutting a single crystal along a (100) plane and rotating about common [001] axis by 36.87°, with no expansion. The four curves corresponding to these four limits are denoted by diamonds, triangles, circles, and asterisks, respectively.

The values of the heat of segregation for both the CS and NCS sites between the fully relaxed boundary (diamond) and the totally unrelaxed boundary (asterisk) are quite different for all three alloys. In some cases, such as the CS and NCS sites in Au-Pd alloys and the CS sites in Ag-Au alloys, relaxation changes the sign of the heat of segregation. The major effect of relaxation, however, comes from the expansion of the boundary. Such an expansion of the grain boundary is simply to release the uniaxial compression, which results from creating the grain boundary at fixed volume, i.e., the change in heat of segregation due to expansion is a mechanical work term. Therefore, it may be concluded that if the grain boundary has a positive excess volume, the magnitude and sign of the segregation may be changed significantly if segregation occurs at fixed volume. The relaxation with respect to the atomic positions and concentrations also changes the value of the heat of segregation, but these effects are not as important as the relaxation with respect to boundary expansion. For the alloys of Cu-Ni and Ag-Au, the difference of the heat of segregation between the segregated (fully relaxed) and the unsegregated boundary is small, implying that the interactions between solute atoms are not very significant in these alloys. However, in Au-Pd alloys this difference is quite substantial. Therefore, the relaxation of the boundary with respect to expansion, atomic positions, and concentrations may all be very important and necessary. However, in some cases,

where the interactions between solutes is not significantly different from that between solute-solvent and solvent-solvent, the effect of relaxation with respect to the atomic concentrations may be ignored.

Classical theories of segregation, such as the Langmuir-McLean and Fowler-adsorption models, are based on approximations to the heat of segregation $Q_i(= \partial F/\partial C_i - \partial F/\partial C_B)$ on the layer adjacent to the grain boundary. As we discussed above, the heat of segregation in the Langmuir-McLean model Q is a *constant*, while for the Fowler model, Q is a linear function of the surface concentration. From the fully relaxed heat of segregation curves (see the diamonds in Figs. 10–12), and the C_1 versus C_B curves in figure 2, we see that neither Q_C nor Q_N are constants, and neither is a linear function of C_1 for all the three alloys. Therefore, the Langmuir-McLean formula and the Fowler-adsorbtion model are not adequate descriptions of the grain boundary segregation found in the present study.

5. Conclusions

Atomistic simulations of segregation to [001] Σ5 twist boundaries in Cu-Ni, Au-Pd, and Ag-Au alloy systems have been performed for a wide range of temperatures and compositions within the solid solution region of these alloy phase diagrams. In addition to the grain boundary segregation profiles, grain boundary free energies, enthalpies, and entropies were determined. These simulations were performed within the framework of the free energy simulation method, in which an approximate free energy functional is minimized with respect to atomic coordinates and atomic site occupation. For all alloy bulk compositions ($0.05 \leq C \leq 0.95$) and temperatures $400 \leq T(\mathrm{K}) \leq 1,100$) examined, Cu and Au segregates to the boundary in the Cu-Ni and Au-Pd alloy systems, respectively; although in the Ag-Au alloys, the majority element segregates to the boundary. The width of the segregation profile is limited to approximately three to four (002) atomic planes. The classical theories for the segregation and the effects of the relaxation with respect to either the atomic positions or the atomic concentrations are discussed. The boundary thermodynamic properties depend sensitively on the magnitude of the boundary segregation.

Acknowledgments

We gratefully acknowledge the Division of Materials Science of the Office of Basic Energy Sciences of the United States Department of Energy (DOE BES DMS), Grant #FG02-88ER45367 for its support of this work. The work of R. LeSar was performed under the auspices of the U.S. Department of Energy and was also supported, in part, by DOE BES DMS.

References

1. E. D. Hondros and M. P. Seah, Int. Met. Rev. **22**, 267 (1977)
2. D. McLean, *Grain Boundaries in Metals* (Clarendon Press, Oxford, 1957).
3. S. Brunauer, P. H. Emmett, and E. Teller, Am. Chem. Soc. **62**, 1723 (1938).
4. M. P. Seah and E. D. Hondros, Proc. R. Soc. London Ser. A. **335**, 1991 (1973).
5. S. Hoffmann, in *Surface Segregation Phenomena*, edited by P.A. Dowben and A. Miller (CRC Press, Boca Raton, FL, 1990), 107.
6. V. Vitek and G.J. Wang, J. Phys. (Paris) **43**, C6–147 (1982).
7. H.Y. Wang, R. Najafabadi, D.J. Srolovitz, and R. LeSar, Phil. Mag. **65**, 625 (1992).
8. R. Najafabadi, H.Y. Wang, D.J. Srolovitz, and R. LeSar, Acta Metall. Mater. **39**, 3071 (1991); (*a*) Mat. Res. Soc. Symp. Proc. **213**, 51 (1991).
9. H.Y. Wang, R. Najafabadi, D.J. Srolovitz, and R. LeSar, Mat. Res. Soc. Symp. Proc. **209**, 219 (1991).
10. H.Y. Wang, R. Najafabadi, D. J. Srolovitz, and R. LeSar, Phys. Rev. B **45**, 12028 (1992).
11. S.M. Foiles, M.I. Baskes, and M.S. Daw, Phys. Rev. B **33**, 7983 (1986).
12. J.W. Gibbs, *Collected Works*, vol. 1 (Yale University Press, New Haven, CT, (1948)